Pressure ranges of velocity splitting of ablated particles produced by pulsed laser deposition in different inert gases*

Ding Xue-Cheng(丁学成), Wang Ying-Long(王英龙)†, Chu Li-Zhi(褚立志), Deng Ze-Chao(邓泽超), Liang Wei-Hua(梁伟华), and Fu Guang-Sheng(傅广生)

College of Physics Science and Technology, Hebei University, Baoding 071002, *China*

(Received 3 September 2012; revised manuscript received 26 December 2012)

The transport of ablated particles produced by single pulsed-laser ablation is simulated via Monte Carlo method. The pressure ranges of velocity splitting of ablated particles in different inert gases are investigated. The result shows that the range of velocity splitting decreases with the atomic mass of the ambient gas increasing. The ambient gas whose atomic mass is more than that of Kr cannot induce the velocity splitting of ablated particles. The results are explained by the underdamping model and the inertia flow model.

Keywords: ablated particles, pressure ranges, velocity splitting, gas type

PACS: 52.65.–y, 52.25.Fi **DOI:** 10.1088/1674-1056/22/8/085202

1. Introduction

Pulsed laser deposition (PLD) has become a popular nanotechnology used to fabricate various nanomaterials.[1–3] The PLD process can be classified into three separate regimes: (i) interaction of laser beam with the Si-target material, resulting in the evaporation of the surface layers and ejection of the ablated particles, (ii) transport of ablated particles in an inert gas, resulting in the formation of nanoparticles, and (iii) diffusion of as-formed nanoparticles with rather low kinetic energy, resulting in the deposition of thin films on the substrate. We focus on the second regime because the vapor nucleation and growth of nanoparticles and velocity splitting of the ablated particles are produced in this regime. The study of transport dynamics of ablated particles in an inert is very important issue in PLD.[4–6] During the transport of ablated particles, the velocity splitting, in which the ablated particles split into the distinct slow and fast components, has received much attention,[7–10] because it affects the size and the density distributions of the nanoparticles. Clarifying the dynamic mechanism and finding the pressure range of the velocity splitting are helpful to realize the controllable preparation of nanoparticles. The dynamic mechanism of the velocity splitting has been investigated by us via Monte Carlo simulation.[9] The result shows whether the splitting appears is determined by the releasing way of the driving force acting on the ablated particles. If the velocity range of driving force of the ablated particles obviously decreases with oscillation, the splitting is likely to be observed; otherwise, it cannot be observed. The velocity splitting can appear only in a certain pressure range and vary with the ambient gas type. A very few studies of velocity splitting at different pressures have been reported. Wood *et al.*[7] found the velocity splitting appears at the pressures of 13-, 17-, 23-, 27-, and 32-Pa He gas. However, we have found any report neither on a certain value of the pressure range, nor on the relation between ambient gas type and pressure range of the velocity splitting of the ablated particles produced by pulsed laser deposition.

In this paper, the transport of the ablated particles produced by PLD is simulated. The pressure range of velocity splitting of the ablated particles is investigated and the value of the pressure range is given.

2. Model and method

The ablated silicon particles include atoms, ions, electrons, clusters, etc., thus transport dynamics of the ablated particles is very complicated. Some assumptions are adopted in our simulation: i) the ablated particle possesses the same mass and radius as Si atom; ii) the initial time corresponds to that the ablated particles just leave out of the edge of Knudsen layer. And then, the ablated particles are uniformly distributed within a cylindrical space of the laser spot diameter. The initial velocities of the ablated particles satisfy the Maxwell–Boltzmann distribution;[11] iii) the ablated particles and the ambient atoms can interact in a manner the same as elastic hard-sphere scattering with a total collision cross section σ_{ab}, which is independent of the scattering angle and $\sigma_{ab} = \pi(r_a + r_b)^2$, where r_a and r_b are the radii of the colliding particles.[9,12] The nucleation and the growth of nanoparticles are not considered, and the inpefectly elastic collisions are ignored. The post-velocities of the colliding particles are written

*Project supported by the National Basic Research Program of China (Grant No. 2011CB612305) and the Natural Science Foundation of Hebei Province, China (Grant Nos. E2012201035 and E2011201134).

†Corresponding author. E-mail: hdwangyl@hbu.edu.cn

© 2013 Chinese Physical Society and IOP Publishing Ltd

with conservation of momentum and energy as,

$$\boldsymbol{V}_{\rm af} = \boldsymbol{c}_{\rm m} + m_{\rm b}/(m_{\rm a}+m_{\rm b})\boldsymbol{c}_{\rm rf}, \quad (1)$$

$$\boldsymbol{V}_{\rm bf} = \boldsymbol{c}_{\rm m} + m_{\rm a}/(m_{\rm a}+m_{\rm b})\boldsymbol{c}_{\rm rf}, \quad (2)$$

in which

$$\boldsymbol{c}_{\rm rf} = \boldsymbol{c}_{\rm r}\left[(\sin\theta\cos\alpha)\hat{x} + (\sin\theta\sin\alpha)\hat{y} + \cos\theta\hat{z}\right]. \quad (3)$$

Here, θ is the scattering angle from 0 to π, and α is obtained from a uniform distribution in a range from 0 to 2π, $\boldsymbol{c}_{\rm r}$ and $\boldsymbol{c}_{\rm rf}$ are the relative velocities before and after a collision respectively, $\boldsymbol{c}_{\rm m}$ is the centre-of-mass velocity of a pair of colliding particles.[12,13]

The region is classified into a series of cells with sizes less than the mean free path of the ambient gas. Simulated paticles are only allowed to collide between each other within the same cell. A pair of colliding particles is selected in the same cell by the acceptance–rejection method. The time of each collision can be calculated by the following formula

$$\Delta t = \frac{2}{N\pi d^2 nc}, \quad (4)$$

where N is the number of ablated particles in this cell, n is the number density of this cell, and $d = r_{\rm a} + r_{\rm b}$ is collision radius.

3. Results and discussion

We consider the ablations of silicon (Si) target in the different gases at various pressures by a KrF excimer laser with a laser fluence of 3.0 J/cm^2, wavelength of 248 nm, and pulse duration of 15 ns. When the ablated particles just leave out of the Knudsen layer, the density, the radial velocity, and the

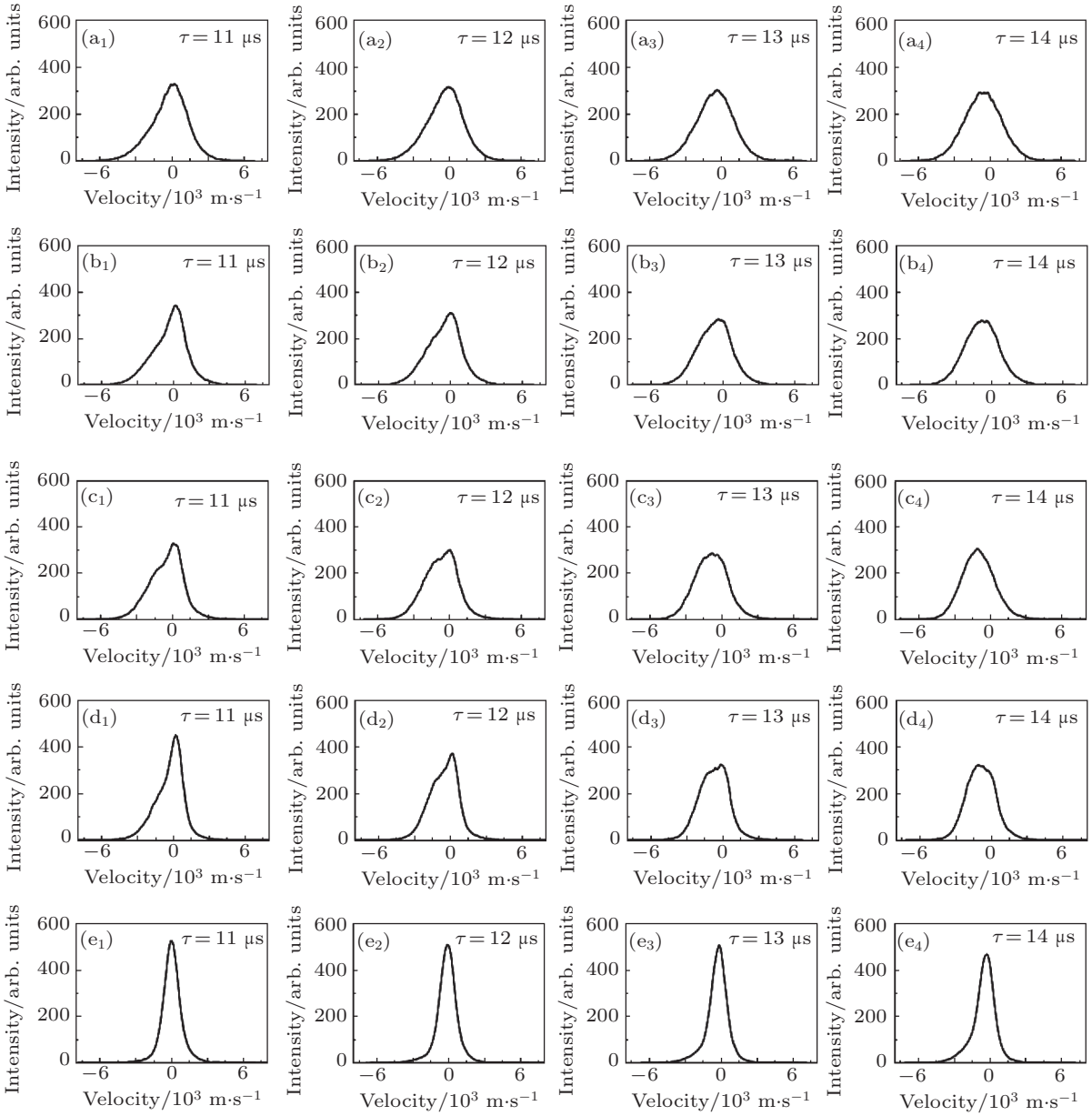


Fig. 1. The time evolutions of the radial velocity distribution in Ar ambient, where panels (a$_1$)–(a$_4$), (b$_1$)–(b$_4$), (c$_1$)–(c$_4$), (d$_1$)–(d$_4$), and (e$_1$)–(e$_4$) correspond to the pressures of 40, 50, 90, 150, and 180 Pa, respectively.

total number of ablated particles are 1.66×10^{26} m^{-3}, 1760 m/s, and 1.01×10^{15}, respectively.[12] The time evolutions of the radial velocity distribution in Ar ambient gas are shown in Fig. 1, where panels (a_1)–(a_4), (b_1)–(b_4), (c_1)–(c_4), (d_1)–(d_4), and (e_1)–(e_4) correspond to the pressures of 40, 50, 90, 150, and 180 Pa, respectively. Only one cycle of splitting is observed under the pressures of 50, 90, and 150 Pa, separately, but the splitting does not appear under a pressure of 40 Pa nor under a pressure 180 Pa. The pressure range of velocity splitting of ablated particles in Ar ambient is from 50 Pa to 150 Pa. The plots of velocity peak position versus time are shown in Fig. 2. Under a cartain pressure, the velocity of the peak position decreases with time increasing. With the increase of the pressure of ambient gas, the velocity variation range first increases and then decreases. For a given pressure, the full width at half maximum (FWHM) of radial velocity curve dicreases with time increasing. With the increase of the pressure of ambient gas, the variation range of the full width at half maximum first increases and then decreases (Fig. 3). The variation ranges of the peak position and the full width at half maximum for observing splitting are greater than those for the case of no splitting. Whether the velocity splitting is observed is determined by the releasing mechanism of the driving force acting on the ablated particles. Only when the driving force decreases in an oscillatory way, can the velocity splitting be observed.[9] The environment provides the drag force for the ablated particles, which varies with time and position. In the "average" sense, the "average" drag force determines releasing way of driving force. If the "average" drag force is very small, so that it can be ignored, the ablated particles are in a state of free-like motion. When the "average" drag force is smaller, releasing mechanism of driving force presents an oscillatory decrease due to the underdamping. For a bigger drag force, it decreases monotonically, owing to overdamping. According to Yoshida's model, the drag force acting on the ablated particles is proportional to the ambient gas density.[14] The ambient gas density increases with presessure increasing. When the pressure of Ar gas is under 50 Pa–150 Pa, the drag force is smaller, the driving force decreses in an oscillatory way, and the splitting can be observed.

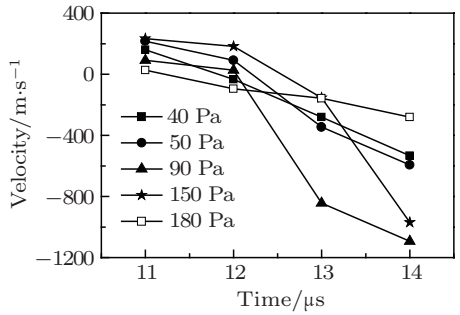


Fig. 2. Time evolutions of velocity peak position at some different pressures.

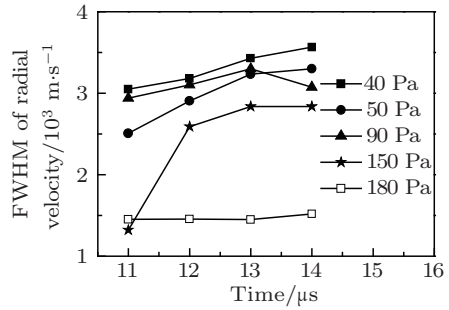


Fig. 3. Time evolutions of full width at half maximum of radial velocity at some different pressures.

The transport dynamic behaviors of ablated particles in He, Ne, Dum, Ar, and Kr gases at various pressures are simulated, in which Dum gas is a dummy gas which has the same atomic mass and radius as Si atom. The results demonstrate that the velocity splitting of the ablated particles can appear only in a certain pressure range varying with the ambient gas type. The pressure ranges in various gases are shown in Table 1. Obviously, the ambient gas whose atomic mass is more than that of Kr cannot induce velocity splitting of ablated particles. As ambient atomic mass decreases, minimal pressure at which the splitting appears is approximately constant ($\sim$ 50 Pa), while the maximal pressure increases. In Monte Carlo simulation, the ambient atom that participates in collisions possesses two crucial parameters: mass and radius. Compared with atomic radius, the atomic mass is dominative for the collision due to its wider varying range. For the ambient gas with heavier atoms, the lower pressure can induce the higher drag force. Thus pressure range inducing splitting decreases with atomic mass increasing.

Table 1. Pressure ranges of velocity splitting of ablated particles in different ambient gases.

Ambient gases	He	Ne	Dum	Ar	Kr
Atomic mass/u	4.0026	20.197	28.086	39.948	83.8
Atomic radius/nm	0.032	0.069	0.111	0.097	0.112
Pressure range/Pa	60–4000	40–400	40–220	50–150	no splitting

The velocity splitting at pressures lower than 60 Pa can be found in Ref. [7]. Their experimental data include the nucleation and growth. In the presence of the nucleation and growth, the pressure at which velocity splitting can occur is lower than in the absence of nucleation and growth.

4. Conclusion

The transports of the ablated particles produced by PLD in He, Ne, Dum, Ar, and Kr gases at various pressures are simulated. The pressure ranges of velocity splitting in different inert gases are given, which decrease with ambient atom mass increasing. The ambient gas whose atomic mass is more than that of Kr cannot induce the velocity splitting of ablated particles. The appropriate pressure can result in the underdamped oscillation of the driving force, and the velocity splitting is observed.

References

[1] Lownds D H, Geohegan D B, Puretzky A A, Norton D P and Rouleau C M 1996 *Science* **273** 898

[2] Wang Y L, Chen C, Ding X C, Chu L Z, Deng Z C, Liang W H and Fu G S 2011 *Laser Part. Beams* **29** 105

[3] Kim K H, Watanabe K, Mulegeta D, Freund H and Menzel D 2011 *Phys. Rev. Lett.* **107** 047401

[4] Amorusoa S, Bruzzese R, Wang X and Xia J 2008 *Appl. Phys. Lett.* **92** 041503

[5] Huang Q and Chen J 2009 *Appl. Phys. Lett.* **95** 191104

[6] Wang Y L, Chu L Z, Li Y L and Fu G S 2009 *Micro & Nano Lett.* **4** 39

[7] Wood R F, Chen K R, Leboeuf J N, Puretzky A A and Geohegan D B 1997 *Phys. Rev. Lett.* **79** 1571

[8] Harilal S S, Binghu C V, Tillack M S, Najmabadi F and Gaeris A C 2003 *J. Appl. Phys.* **93** 2380

[9] Ding X C, Wang Y L, Chu L Z, Deng Z C, Liang W H, Galalaldeen I I A and Fu G S 2011 *Europhys. Lett.* **96** 55002

[10] Ding X C, Fu G S, Liang W H, Chu L Z, Deng Z C and Wang Y L 2010 *Acta Phys. Sin.* **59** 3331 (in Chinese)

[11] Leonid V Z and Barbara J G 1997 *Appl. Phys. Lett.* **71** 551

[12] Han M, Gong Y, Zhou J, Yin C, Song C F, Muto N, Takiya T and Iwata Y 2002 *Phys. Lett. A* **302** 182

[13] Bittencurt J A 2004 *Fundamentals of Plasma Physics* (New York: Springer-Verlag) pp. 560–566

[14] Yoshida T, Takeyama S, Yamada Y and Mutoh K 1996 *Appl. Phys. Lett.* **68** 1772